

VENUGOPAL PALANISWAMY<sup>1</sup>  
KALIAPPAN SEENIAPPAN<sup>2</sup>  
THANIGAIVELAN  
RAJASEKARAN<sup>3</sup>  
NATRAYAN LAKSHMAIYA<sup>4</sup>

<sup>1</sup>Department of Mechanical Engineering, Muthayammal College of Engineering, Rasipuram, Namakkal (Dt), Tamil Nadu, India

<sup>2</sup>Department of Mechanical Engineering, Velammal Institute of Technology, Tamil Nadu, Chennai, India

<sup>3</sup>Department of Mechanical Engineering, AKT Memorial College of Engineering and Technology, Kallakurichi, Tamil Nadu, India

<sup>4</sup>Department of Mechanical Engineering, Saveetha School of Engineering, SIMATS, Tamil Nadu, Chennai., India

SCIENTIFIC PAPER

UDC 544.5/.6:621

## ENHANCING MRR AND ACCURACY WITH MAGNETIZED GRAPHITE TOOL IN ELECTROCHEMICAL MICROMACHINING OF COPPER

### Article Highlights

- The effect of graphite and magnetized tool in EMM is reported
- Electro-magnetized graphite tool electrode shows a higher machining rate and lower overcut
- Graphite electrode produces an 11.9% reduced overcut

### Abstract

*Micro hole is the fundamental feature found in any device and its components. Hence this paper aims to produce the micro holes using electrochemical micromachining (EMM). The existing machining techniques in EMM for creating micro holes are associated with more overcut (OC). Hence, reducing OC and enhancing the machining rate (MR) is essential. This paper aspires to investigate the effect of the graphite electrode with magnetic force on the copper plate. Four different tools, namely the electromagnetic graphite tool (EMGT), permanent magnet graphite tool (PMGT), graphite tool, and stainless steel (SS) tool, are employed for these experiments. The major influencing factors are machining voltage in volts, duty cycle in % and electrolyte concentration in g/l was considered on MR and OC. The results revealed that EMGT, PMGT, and graphite electrodes produce MR of 106.4%, 74.6 % and 44.5 % over the SS tool at a parameter level of 23 g/l, 15 V, and 85%, respectively. Furthermore, graphite and EMGT electrodes resulted in 11.9% and 3.41% reduced OC, respectively, than the SS tool at parameter levels of 8 V, 95% and 28 g/l. Additionally, the scanning electron microscope (SEM) picture examination is conducted to identify the magnetic field effect on the work surface.*

*Keywords: electrode, electromagnet, coating, machining rate, overcut.*

Copper, one of the finest ductile nature materials. is appropriate material for manufacturing power circuit boards, automobile parts, and medical and biomedical components. Due to its crystalline nature, the copper material produces more burrs while machining through conventional technology due to the tool structure,

rotational speed and cutting forces [1,2]. On the other hand, among various techniques in unconventional methods, EMM provides the right solutions for the problems stated above due to its advantages characteristics such as non-contact machining, no tool wear, high precision and excellent surface finish etc., [3,4]. To enhance the machining rate, researchers worldwide followed various strategies in EMM. Sharma *et al.* [5] studied the EMM performance with different pulsed voltages to obtain high accuracy and machining rate on stainless steel workpieces. They employed the various waveforms of pulsed current, such as rectangular, sinusoidal, triangular and half-wave rectified power supplies. Among these waveforms,

Correspondence: T. Rajasekaran, Department of Mechanical Engineering, AKT Memorial College of Engineering and Technology, Kallakurichi, Tamil Nadu, India-606 202.

E-mail: [tvelan10@gmail.com](mailto:tvelan10@gmail.com)

Paper received: 31 July, 2022

Paper revised: 11 October, 2022

Paper accepted: 14 October, 2022

<https://doi.org/10.2298/CICEQ220731027P>

triangular improves accuracy. Bian *et al.* [6] attempted with five different electrodes, namely SS, aluminium alloy, brass, tungsten and steel, to realize the influence of tool materials on the EMM performance. The stray current effect in the machining zone was slowed down while using aluminium alloy due to the formation of oxide layers on the electrode surface. These oxide layers act as side insulation attributes for lesser OC. Also, micro holes' machining rate and quality are 3 times better with aluminium alloy than other materials. Zhan *et al.* [7] have generated gas bubbles around the electrode to provide an insulating effect in the EMM process. These generated gas bubbles remove the machined products quickly, stabilize the current flow, and improve the machining rate by 2.6 times over normal EMM processes. Rajkeerthi *et al.* [8] employed  $\varnothing$  300  $\mu$ m fabricated hollow tool in the EMM process on the nickel-based superalloy. The MR and OC improved by 2.04% and 24.57%, respectively for the fabricated hollow tool. Kunar *et al.* [9] have improved micro-hole accuracy by applying rectangular waveform voltage in the EMM process on SS 304 work material with masked tool electrodes. Soundarrajan *et al.* [10] employed hot air in the EMM process to study the effect of electrolyte temperature on the copper work material. The results reveal that using citric acid for the copper work materials produces the non-conductive dissolved products surrounding the tool and create the insulating effect for improving micro-hole accuracy. Mouliprasanth *et al.* [11] tried different electrolytes for machining shape memory alloy in EMM with SS electrodes. Among those electrolytes, passivating electrolyte shows a higher machining rate than the non-passivating electrolyte. Shanmugam *et al.* [12] fabricated the stainless-steel electrode through additive manufacturing and used it in the EMM process to study its effects on titanium alloy. The machining parameters such as voltage, concentration and duty cycle are varied on the MR, OC and conicity. They noted the improved OC and conicity with the fabricated tool due to the higher molecular bond than the normal electrode. Liu *et al.* [13] have used novel silver-coated glass tube electrodes to control the stray current effect in the EMM process. Yang *et al.* [14] conducted the EMM experiments with hollow electrodes with a vibrating workpiece at a 1.5 Hz frequency to ensure the continuous removal of machined products. The uniform current flow and distribution in the machining zone due to the workpiece's vibration contribute to a high-precision micro hole. Pradeep *et al.* [15] investigated the EMM process parameters with graphite electrodes for SS 304 work material. They compared the results of graphite electrodes to the cryogenically treated tool and normal electrodes. The surface of micro holes was noted with fewer stray cuts while using cryogenically

treated electrodes than other electrodes. Arul *et al.* [16] have utilized square shape composite electrodes in the EMM for the copper work material. The composite square tool produces sharp corners than normal stainless-steel electrodes while machining rectangular slots. Gopinath *et al.* [17] conducted experiments on a titanium alloy with the assistance of a magnetic field using the EMM process. They noted 68%, 47%, and 55% improvement in the MR, OC and surface roughness, respectively, for magnetic field-assisted machining compared to non-magnetic machining. Palani *et al.* [18] studied the suitability of electrode material in the EMM process for a nickel-based alloy. The materials, such as copper, tungsten and brass, are considered electrode materials, and the response surface methodology technique has been employed to understand the relation between the process variables and responses. They noted that copper and tungsten produce the improved MR and OC, respectively, compared to the brass electrode. Liu *et al.* [19] studied the EMM process through a helical electrode with a jet electrolyte. This type of electrode hinders the stray current corrosion near the micro holes. Patel *et al.* [20] tried the flexible electrode in The EMM process to fabricate the micro texture on the SS 304 work material. They created the curvatures in the electrode to increase the machining zone's current density. Soundarrajan *et al.* [21] studied the influence of different electrode coating on copper work material through The EMM process. The length of the tool and coating thickness significantly affects the machining performance.

Saravanan *et al.* [22] studied the ultraviolet rays and magnetic field coupled effect on the EMM performances and employed various optimization techniques, such as TOPSIS, VIKOR and GRA. Vats *et al.* [23] examined the EMM performance using different electrolyte temperatures on Inconel alloy and noted a 4-19% improvement in the MR at 40 °C. Vinod Kumar *et al.* [24] studied the EMM process using a magnetic field on a SS 316 work material. They found a 1.82 times higher MR over the normal EMM process. Geethapiriyam *et al.* [25] conducted experiments using a nickel-coated electrode in the EMM of titanium alloy. They observed a better surface finish and 12% improved OC by nickel-coated tools than the standard electrode. Maniraj *et al.* [26] fabricated a different set-up to heat the electrode and studied the machining characteristics. The heated electrode results in 37 % and 88 % improvement in the OC and MR, respectively. Liu *et al.* [27] have employed non-conductive materials on the tool steel alloy, such as SiO<sub>2</sub> and Si<sub>3</sub>N<sub>4</sub> insulated tools. They noted considerable development in the taper angle of the hole and OC. Guo *et al.* [28] carried out experiments in the EMM on the nickel superalloy through the rotating electrode. The tool rotation speed

instantly pushes out the electrolytic products from the machining zone and causes a higher MR. Mouliprasanth and Hariharan [29] have studied the effect of mixed electrolytes on the ECMM process and found an improvement in machining speed, circularity, conicity, and overcut. Thanigaivelan *et al.* [30] employed different tool tips coated with the epoxy insulation in EMM for machining SS 304. Wang *et al.* [31] adopted the spherical tool in The EMM process to study the effect of tool rotation on the taper angle of the hole and MR. They noticed a 139% reduced taper angle of the hole and a 43% improvement in the MR.

It is clear from the literature mentioned above that researchers have attempted to enhance MR and OC with modified tools. Although many techniques exist, namely tool modifications and insulation, it is still challenging to insulate the tool economically at the micro level. Therefore, in this study, an attempt was made to affect the copper plate with a graphite electrode and magnetic field. Commercially available graphite pencil tips are considered electrodes combined with electromagnetic and permanent magnet effects. Generally, electromagnets and permanent magnets are successfully employed in various sectors, such as biomedical and electronics, for different applications. Although Gopinath *et al.* [17] have applied a magnetic field for machining titanium alloy in EMM, a detailed study is needed to understand the effect of the magnetic field in the EMM process. This magnetic effect could repel the machined product and instantly refresh the electrolyte at the machining zone. Therefore, it is important to investigate the influences of magnetic and non-magnetic graphite tools with SS tools on the EMM performance. The most significant EMM process variables, machining voltage in V, duty cycle in %, and electrolyte concentration in g/l, were considered for the experiment. In addition, the output responses, such as MR and OR, are considered for assessing the EMM performance. Furthermore, SEM image analyses of machined surfaces were done to explore the effect of the magnetic force on micro holes.

## EXPERIMENTAL

The experiments were conducted through an indigenously fabricated EMM set-up. The set-up incorporated different subcomponents, such as tool control arrangement, electrolyte supply system, electrolyte tank and microcontroller system. The workpiece of a 1 mm thick copper plate,  $\varnothing$  500  $\mu$ m SS rod, and commercially available graphite were used as tool electrodes for the experiments. The tools were insulated with epoxy resin to control the stray current, and sodium nitrate ( $\text{NaNO}_3$ ) under different

concentrations was used as an electrolyte. The micro-hole completion was witnessed by the progression of gas bubbles beneath the workpiece. Four different electrodes were used in the experiments. The remaining tools were made of graphite material besides the standard electrode. The electromagnetic tool (EMT) holder was fabricated and energized separately. The commercially available graphite pencil tip was fixed with an EMT holder, which is wound with insulated copper coils of diameter 10 mm. Based on Ampere's law of electromagnetism, the electromagnetic flux was induced by an electric current when it passed through the graphite material. The EMT holder set-up was connected to a separate power supply unit. Also, commercially available ten numbers of round hollow N 52 grade permanent neodymium magnets were used as another tool. The use of permanent magnets produced a constant magnetic flux and electromagnets with varying magnetic flux. The MR was calculated by dividing the thickness of the workpiece by the time taken for machining through the hole. The difference in diameter between the tool electrode (constant) and the top side micro hole was noted to find the OC of the micro hole. The major factors and their range are displayed in Table 1. The plan of experiments was developed according to the method of varying one factor at a time.

Table 1. Machining parameters and their levels.

Machining parameters	Units	Range
Type of Electrode	-	Electromagnetic Graphite Tool (EMGT), Permanent Magnet Graphite Tool (PMGT), Graphite tool and stainless steel (SS) tool
Machining Voltage (MV)	V	8,9,10,11,12
Duty cycle (DC)	%	55,65,75,85,95
Electrolyte concentration (EC)	g/l	20,22,24,26,28
Frequency	Hz	85

## RESULTS AND DISCUSSION

### Effect of machining voltage on MR and OC

Figure 1a presents the dependence of machining voltage on MR for various tool electrodes. It shows that the PMGT electrode produces the highest MR among the tested electrodes. An increase in voltage level increases the MR. The combined magnetic and electrical force of a round magnet increases the MR. The round-shaped magnets constantly induce the magnetic flux in the machining zone. Along with that

electric force in between the inter-electrode gap (IEG) removes the machined product quickly. The quick and continuous removal of machined products leads to a higher MR [32,33]. In the PMGT electrode, the MR is 106.4% higher than the SS tool for the parameter level of 8 V, 95%, and 28 g/l. Also, this value is the maximum MR in all experiments conducted by different types of electrodes. This phenomenon is because the constant magnetic field effects accelerate the displacement of the ions in the electrolyte, which triggers the flow of electricity in addition to other chemical changes [34]. The delocalized electrons in graphite cause its conductivity. A magnetic effect is generated when the current passes through the graphite electrode, surrounded by a permanent magnet. This effect attributes to a rise in the MR over other electrode types. Concerning the EMGT electrode, a discontinuous magnetic flux in the electrolyte is responsible for the next highest MR. In the EMGT, the magnetic flux generation depends on the quantity of voltage supplied to the coil. Generally, the presence of salt in the electrolyte increases the conductivity. Also, the magnetic flux creates the turbulence effect on electrolyte molecules and leads to higher conductivity [35,36]. The EMGT electrode produces a 74.6% higher MR than the SS tool. The graphite tool electrode induces the electrostatic effect when current is passed through it. This phenomenon of electrostatic flux pulls out the machined products from the IEG and machining area. Therefore, the graphite tool electrode produces a 44.5% increased MR over the SS tool. Moreover, the PMGT, EMGT and graphite electrodes produce an

increased MR of 82.04%, 55.5%, and 28.8%, respectively, for the parameter solution of 9 V, 95% and 28 g/l over the SS tool.

Figure 1 (b) displays the influences of voltage over OC for different tool electrodes. As per the graph, the graphite electrode reduces the OC to 258  $\mu\text{m}$  at a parameter solution of 8 V, 95%, and 28 g/l. Moreover, this is the first least OC value in the experiment. The rising level of machining voltage contributes more to the OC. The graphite electrode is made up of a hexagonal molecular structure, and this formation of an atom causes its excellent electrical conductivity. This phenomenon and electrostatic pull-out force are attributed to a lesser OC [37]. The use of EMGT and PMGT produces the next lowest OC. The Graphite tool electrode resulted in an 11.9% lesser OC than the standard SS tool electrode. The EMGT electrode creates the second lesser OC (283  $\mu\text{m}$ ), which is 3.41% lower than the SS tool for similar parameters. Also, the PMGT electrode generates OC of 292  $\mu\text{m}$ , which is 3.03% lesser than the SS tool. In this, EMGT takes slight edge improvement than PMGT electrode. The round-shaped permanent magnet swirls the electrolyte molecules rapidly in the machining zone, leading to the dissolution of the excess materials with PMGT than EMGT electrode [38]. As a result, the graphite, EMGT, and PMGT electrodes produce an OC of 302  $\mu\text{m}$  (i.e. 39.2% enhancement), 311  $\mu\text{m}$  (i.e. 8.48% enhancement), and 320  $\mu\text{m}$  (i.e. 5.76% enhancement), respectively, at the parameter combination of 8 V, 95% and 28 g/l compared to the SS tool.

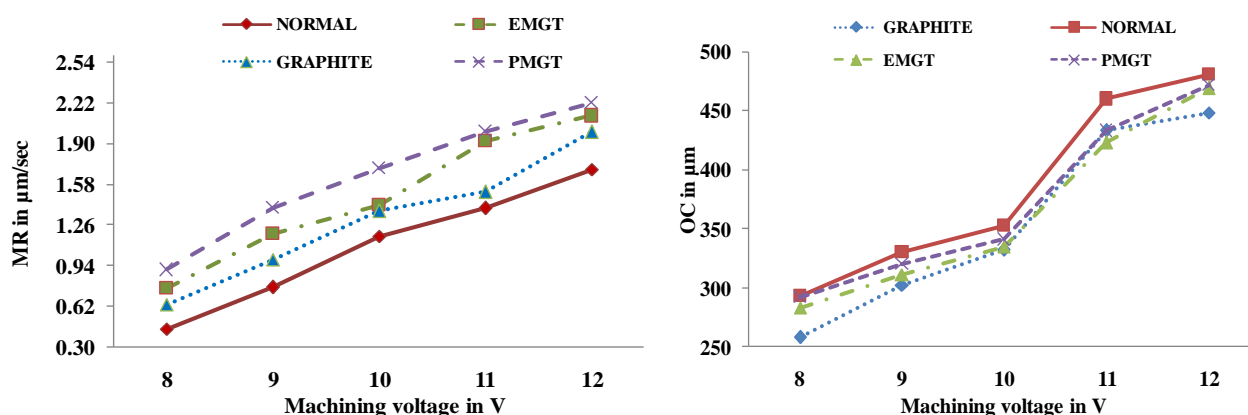


Figure 1. Influence of machining voltage on (a) MR and (b) OC.

### Effect of duty cycle on MR and OC

Figure 2a represents the influence of the duty cycle over the MR for all four tool electrodes. The graph infers that the PMGT electrode produces the highest MR than other tools, and the MR increases with respect to the duty cycle. The increase in the duty cycle induces the electrochemical reaction and generates hydrogen

bubbles near the electrode due to the application of permanent magnets [38]. The higher formation of hydrogen bubbles contributes to the higher bubbles diffusions, which attribute to the micro-moving force, leading to the quick refreshment of the electrolyte and a fast electron movement [27]. Thus, the PMGT electrode generates a 61.76% elevated MR compared

to the SS tool at the parametric levels of 55%, 12 V, and 28 g/l. The next maximum MR is attained with the EMGT electrode, which generates a 39.92% higher MR than the SS tool. The graphite electrode contributes the second highest MR, which is 21.8% higher than the SS tool. These PMGT, EMGT, and graphite tool electrodes produce the maximum MR, i.e. 97.8%, 67.5%, and 61.9% higher than the SS tool, respectively, at the parameter levels of 65%, 12 V, and 28 g/l.

Figure 2b illustrates the influences of the duty cycle on the OC for various tool electrodes. The graphite electrode enlarges the OC to 289  $\mu\text{m}$  for 55%, 12 V, and 28 g/l. In general, due to the electrochemical and magnetic effect, the electrolyte temperature rises in the machining zone to a certain extent. These temperature changes create a good bonding between the graphite electrode surface and epoxy coating [39]. Hence, this phenomenon arrests the stray current and confines the current flow attributing to a lesser OC than others. The EMGT and PMGT electrodes generate the next lesser OC, i.e. 307  $\mu\text{m}$  and 319  $\mu\text{m}$ , respectively than the SS tool for the same parameter level. The EMGT and PMGT electrodes produce 10.14% and 7.89% lower OCs than the SS tool. In addition, at the

parametric level of 65%, 12 V, and 28 g/l, the graphite, EMGT, and PMGT electrodes generate lower OC of 390  $\mu\text{m}$  (i.e. 10.1%), 395  $\mu\text{m}$  (i.e. 8.99%) and 390  $\mu\text{m}$  (i.e., 10.1%) respectively than the SS tool. SEM images in Figure 3 (a–b) present the micro hole machined with different electrodes, such as the EMGT and PMGT, for the parameters 55%, 12 V, and 28 g/l. The graphite electrode shows good-quality holes, and the magnetic field effect shows unnecessary material erosion over the edge of the micro-hole. Figure 3a shows the electromagnetic effect of disproportionate material removal on the circumference compared to the PMGT, as shown in Figure 3b.

**Effect of electrolyte concentration on MR and OC**

Figure 4a presents the influences of the electrolyte concentration on the MR using various tool electrodes, and the MR increases with the electrolyte concentration. The PMGT electrode generates the maximum MR among the electrodes because the graphite electrodes undergo a galvanic chemical reaction in the electrolyte solution [40].

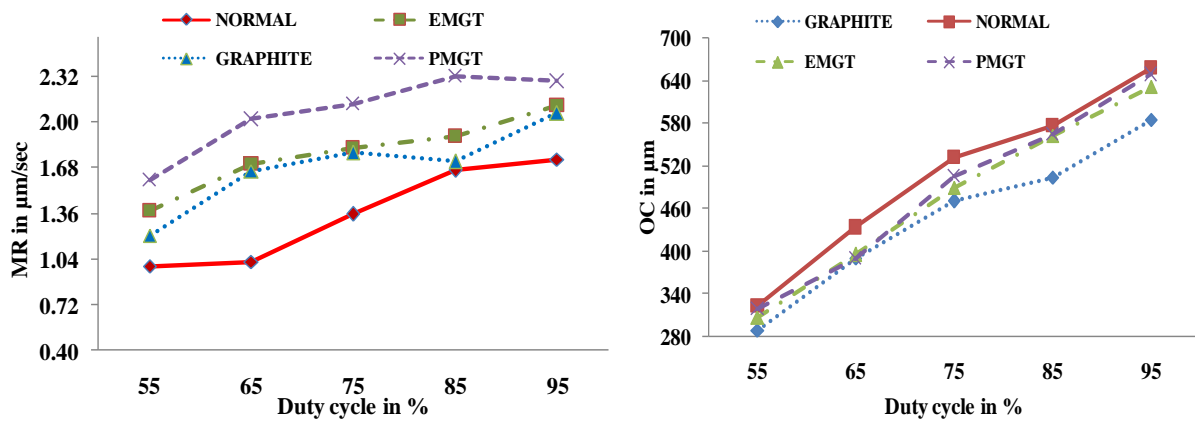


Figure 2. Influence of duty cycle on (a) MR and (b) OC.

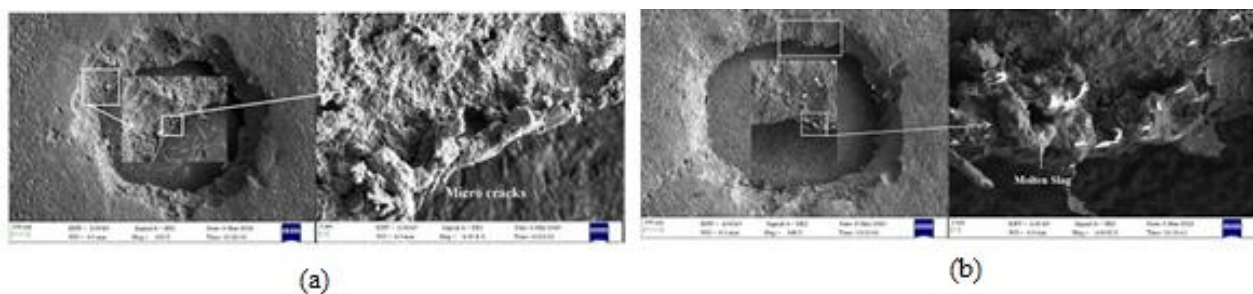


Figure 3. SEM image of micro holes machined at 55%, 12 V, and 28 g/l for (a) EMGT and (b) PMGT.

In the PMGT electrode, the positive and negative polarization galvanic reaction occurs at the IEG, leading to a high MR. During this reaction, the chance for adherence of sludge to the graphite electrode surface is more [41]. In addition, with magnetic Lorentz force, the PMGT electrode produces a 104% maximum MR compared to the SS tool for the parameter levels of 20 g/l, 12 V, and 95%. The EMGT electrode exhibits the next highest MR for a similar parameter level. The EMGT electrode contributes 86.9% higher MR than the SS tool. The MR for the graphite tool electrode is 77.2% higher than for the SS tool. Furthermore, at the parametric levels of 22 g/l, 12 V, and 95%, PMGT, the EMGT and graphite electrodes show 97.8%, 78.5%, and 38.5% higher MR compared to the SS tool.

Figure 4b shows the influence of the electrolyte concentration on the OC for various tools. The graphite, EMGT, and PMGT electrodes generate the OC of

177  $\mu\text{m}$ , 182  $\mu\text{m}$ , and 188  $\mu\text{m}$ , respectively, for the parameter levels of 22 g/l, 12 V, and 95%. Moreover, these OC values are the lowest among the conducted experiments [15]. The graphite electrode shows a 15.02% lesser OC than the standard SS tool. Figure 5a portrays the micro holes fabricated with the graphite electrodes. The figure clears that circumference of the micro holes is precise, and there is less etching surface due to the confined current distributions on the machining area. The SEM micrograph presented in figure 5 (b) shows the micro-hole fabricated with EMGT at the parameter level of 20 g/l, 12 V, and 95%. The over-etching surface is witnessed on its circumference. The PMGT electrode offers the next lowest OC. Hence, in the PMGT electrode, the OC is 10.6% lower than that of the SS tool. Figure 5c presents the micro-hole fabricated through the PMGT electrode. Figure 5 (d) shows the micro-hole surface machined using the SS tool at 20 g/l, 12 V, and 95%.

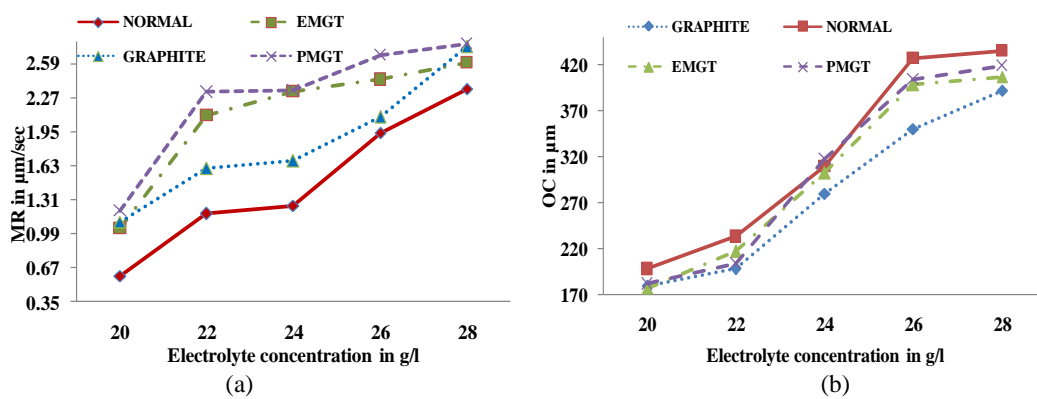


Figure 4. Influence of electrolyte concentration on (a) MR and (b) OC.

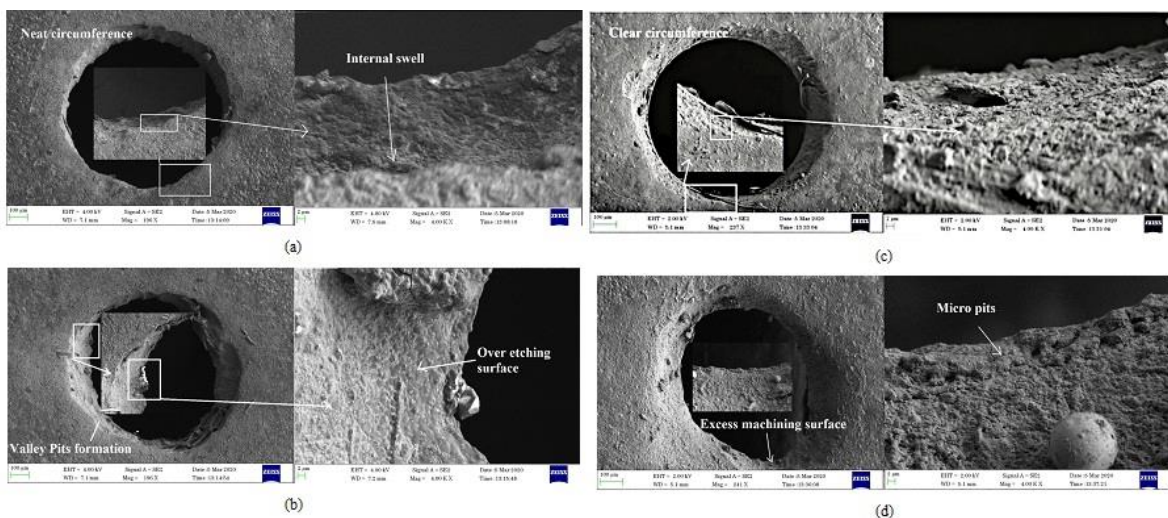


Figure 5. SEM image of micro holes machined at 20 g/l, 12 V and 95% for (a) Graphite, (b) EMGT, (c) PMGT, and (d) SS tool.

## CONCLUSION

Four different electrodes, such as the EMGT, PMGT, graphite, and SS tool, are used for the experiments. The experimental results show that the PMGT electrode produces a 106.4% higher MR than the standard SS tool for the parameter solution of 8 V, 95%, and the EMGT electrode of 74.6% shows 28 g/l and the next highest MR. The graphite tool electrode produces a 44.5% increased MR compared to the SS tool electrode due to the electrostatic effect. The graphite tool electrode resulted in an 11.9 % lesser OC than the SS tool. The EMGT electrode creates the second lesser 283  $\mu\text{m}$  OC, which is 3.41 % lower than the SS tool for the parameter solution of 8 V, 95% and 28 g/l. Based on the investigation, the PMGT and EMGT electrodes are recommended where the MR is in demand, and the graphite electrode could be chosen for enhancing the accuracy. Further experiments can be planned, such as different tool electrode materials and magnetic fields.

## ACKNOWLEDGEMENT

This dataset is the outcome of the experiments carried out in the Department of Mechanical Engineering, Muthayammal Engineering College, Rasipuram, India. The authors are also thankful for all the support the institution provides.

## REFERENCES

- [1] X. Wu, L. Li, N. He, M. Zhao, Z. Zhan, *Int. J. Adv. Manuf. Technol.* 79 (2015) 321–327. <https://doi.org/10.1007/s00170-015-6828-5>.
- [2] R. Thanigaivelan, R.M. Arunachalam, P. Drukpa, *Int. J. Adv. Manuf. Technol.* 61 (2012) 1185–1190. <https://doi.org/10.1007/s00170-012-4093-4>.
- [3] M. Soundarrajan, R. Thanigaivelan, *Russ. J. Appl. Chem.* 91 (2018) 1805–1813. <https://doi.org/10.1134/S1070427218110101>.
- [4] J.R. Vinod Kumar, R. Thanigaivelan, M. Soundarrajan, *Mater. Manuf. Process.* 37 (2022) 1526–1539. <https://doi.org/10.1080/10426914.2022.2030874>.
- [5] V. Sharma, P. Gupta, J. Ramkumar, *J. Manuf. Process.* 75 (2022) 110–124. <https://doi.org/10.1016/j.jmapro.2022.01.006>.
- [6] J. Bian, B. Ma, H. Ai, L. Qi, *Materials* 14 (2021) 2311. <https://doi.org/10.3390/ma14092311>.
- [7] S. Zhan, Y. Zhao, *J. Mater. Process. Technol.* 291 (2021) 117049. <https://doi.org/10.1016/j.jmatprotec.2021.117049>.
- [8] E. Rajkeerthi, P. Hariharan, N. Pradeep, *Mater. Manuf. Process.* 36 (2021) 488–500. <https://doi.org/10.1080/10426914.2020.1843672>.
- [9] S. Kunar, B. Bhattacharyya, *J. Adv. Manuf. Syst.* 20 (2021) 27–50. <https://doi.org/10.1142/S0219686721500025>.
- [10] M. Soundarrajan, R. Thanigaivelan, *Russ. J. Electrochem.* 57 (2021) 172–182. <https://doi.org/10.1134/S1023193521020117>.
- [11] B. Mouliprasanth, P. Hariharan, *Russ. J. Electrochem.* 57 (2021) 197–213. <https://doi.org/10.1134/S1023193521030095>.
- [12] R. Shanmugam, M. Ramoni, G. Thangamani, M. Thangaraj, *Metals* 1 (2021) 778. <https://doi.org/10.3390/met11050778>.
- [13] G. Liu, H. Tong, Y. Li, H. Zhong, *Precis. Eng.* 72 (2021) 356–369. <https://doi.org/10.1016/j.precisioneng.2021.05.009>.
- [14] T. Yang, X. Fang, Y. Hang, Z. Xu, Y. Zeng, *Int. J. Adv. Manuf. Technol.* 116 (2021) 2651–2660. <https://doi.org/10.1007/s00170-021-07556-8>.
- [15] N. Pradeep, K.S. Sundaram, M. Pradeep Kumar, *Mater. Manuf. Process.* 35 (2020) 72–85. <https://doi.org/10.1080/10426914.2019.1697445>.
- [16] T.G. Arul, V. Perumal, R. Thanigaivelan, *Chem. Ind. Chem. Eng. Q.* 28 (2022) 247–253. <https://doi.org/10.2298/CICEQ210501036A>.
- [17] T.P. Gopinath, J. Prasanna, C.C. Sastry, S. Patil, *Mater. Sci.-Pol.* 39 (2021) 124–138. <https://doi.org/10.2478/msp-2021-0013>.
- [18] S. Palani, P. Lakshmanan, R. Kaliyamurthy, *Mater. Manuf. Process.* 35 (2020) 1860–1869. <https://doi.org/10.1080/10426914.2020.1813888>.
- [19] B. Liu, H. Zou, H. Luo, X. Yue, *Micromachines* 11 (2020) 118. <https://doi.org/10.3390/mi11020118>.
- [20] D.S. Patel, V. Agrawal, J. Ramkumar, V.K. Jain, G. Singh, *J. Mater. Process. Technol.* 282 (2020) 116644. <https://doi.org/10.1016/j.jmatprotec.2020.116644>.
- [21] M. Soundarrajan, R. Thanigaivelan, *Mater. Manuf. Process.* 35 (2020) 775–782. <https://doi.org/10.1080/10426914.2020.1740252>.
- [22] K.G. Saravanan, R. Thanigaivelan, M. Soundarrajan, *Bull. Pol. Acad. Sci.:Tech. Sci.* 69 (2021) e138816. <https://doi.org/10.24425/bpasts.2020.135382>.
- [23] A. Vats, A. Dvivedi, P. Kumar, *Mater. Manuf. Process.* 36 (2020) 677–692. <https://doi.org/10.1080/10426914.2020.1866189>.
- [24] J.R. Vinod Kumar, R. Thanigaivelan, *Mater. Manuf. Process.* 35 (2020) 969–977. <https://doi.org/10.1080/10426914.2020.1750630>.
- [25] T. Geethapiriyam, A.A. Kumar, A.A. Raj, G. Kumarasamy, J.S. John, *IOP Conf. Ser.: Mater. Sci. Eng.* 912 (2020) p.032039. <https://doi.org/10.1088/1757-899X/912/3/032039>.
- [26] S. Maniraj, R. Thanigaivelan, *Mater. Manuf. Process.* 34 (2019) 1494–1501. <https://doi.org/10.1080/10426914.2019.1655153>.
- [27] G. Liu, Y. Li, Q. Kong, H. Tong, H. Zhong, *Precis. Eng.* 52 (2018) 425–433. <https://doi.org/10.1016/j.precisioneng.2018.02.003>.
- [28] C. Guo, Y. Liu, Z. Wei, J. Niu, *Recent Pat. Mech. Eng.* 10 (2017) 51–59. <https://doi.org/10.2174/2212797610666170208142044>.
- [29] B. Mouliprasanth, P. Hariharan, *Exp. Tech.* 44 (2020) 259–273. <https://doi.org/10.1007/s40799-019-00350-y>.
- [30] R. Thanigaivelan, R. Senthilkumar, R.M. Arunachalam, N. Natarajan, *Surf. Eng. Appl. Electrochem.* 53 (2017) 486–492. <https://doi.org/10.3103/S1068375517050143>.
- [31] Y. Wang, Y. Zeng, N. Qu, D. Zhu, *Int. J. Adv. Manuf. Technol.* 84 (2016) 851–859. <https://doi.org/10.1007/s00170-015-7759-x>.
- [32] W.A. Jorgensen, B.M. Frome, C. Wallach, *Eur. J. Surg.*

- 574 (1994) 83–86.  
<https://pubmed.ncbi.nlm.nih.gov/7531030/>.
- [33] D.Y. Wu, J.F. Li, B. Ren, Z.Q. Tian, Chem. Soc. Rev. 37 (2008) 1025–1041. <https://doi.org/10.1039/B707872M>.
- [34] M. Iqbal, M.M. Nauman, F.U. Khan, P.E. Abas, Q. Cheok, A. Iqbal, B. Aissa, Int. J. Energy Res. 45 (2020) 65–102. <https://doi.org/10.1002/er.5643>.
- [35] Y. Lu, Z. Tu, L.A. Archer, Nat. Mater. 13 (2014) 961–969. <https://doi.org/10.1038/nmat4041>.
- [36] Y. Jin, N. Yang, X. Xu, Appl. Therm. Eng. 179 (2020) 115732. <https://doi.org/10.1016/j.applthermaleng.2020.115732>.
- [37] M. Wissler, J. Power Sources 156 (2006) 142–150. <https://doi.org/10.1016/j.jpowsour.2006.02.064>.
- [38] R.C. Cruz Gómez, L. Zavala Sansón, M.A. Pinilla, Exp. Fluids 54 (2013) 1582. <https://doi.org/10.1007/s00348-013-1582-7>.
- [39] O. Sambalova, E. Billeter, O. Yildirim, A. Sterzi, D. Bleiner, A. Borgschulte, Int. J. Hydrogen Energy 46 (2021) 3346–3353. <https://doi.org/10.1016/j.ijhydene.2020.10.210>.
- [40] F. Bellucci, A. Di Martino, C. Liberti, J. Appl. Electrochem. 16 (1986) 15–22. <https://doi.org/10.1007/BF01015979>.
- [41] P. Natarajan, S.S. Karibeeran, P.K. Murugesan, J. Braz. Soc. Mech. Sci. Eng. 43 (2021). 507. <https://doi.org/10.1007/s40430-021-03228-6>.

VENUGOPAL PALANISWAMY<sup>1</sup>  
 KALIAPPAN SEENIAPPAN<sup>2</sup>  
 THANIGAIVELAN  
 RAJASEKARAN<sup>3</sup>  
 NATRAYAN LAKSHMAIYA<sup>4</sup>

<sup>1</sup>Department of Mechanical Engineering, Muthayammal College of Engineering, Rasipuram, Namakkal (Dt), Tamil Nadu, India

<sup>2</sup>Department of Mechanical Engineering, Velammal Institute of Technology, Tamil Nadu, Chennai, India

<sup>3</sup>Department of Mechanical Engineering, AKT Memorial College of Engineering and Technology, Kallakurichi, Tamil Nadu, India

<sup>4</sup>Department of Mechanical Engineering, Saveetha School of Engineering, SIMATS, Tamil Nadu, Chennai., India

## POVEĆAVANJE BRZINE UKLANJANJA MATERIJALA I TAČNOST SA MAGNETIZOVANIM GRAFITNIM ALATOM U ELEKTROHEMIJSKOM MIKROKOMHINIRANJU BAKRA

*Mikro rupe su osnovna karakteristika svakog uređaja i njegovih komponenti. Stoga ovaj rad ima za cilj da proizvede mikro rupe pomoću elektrohemijske mikromašinske obrade. Postojeće tehnike elektrohemijske mikromašinske obrade za pravljenje mikro rupa su povezane sa više preseka. Stoga je smanjenje preseka i povećanje brzine obrade od suštinskog značaja. Ovaj rad teži da se istraži efekat grafitne elektrode sa magnetnom silom na bakarnu ploču. Za ove eksperimente korišćena su četiri različita alata, a to su: alat, alat sa stalnim magnetom, grafitni alat i alat od nerđajućeg čelika. Razmatrani su glavni faktori uticaja na brzinu obrade i presek, kao što su: napon obrade u voltima, radni ciklus u % i koncentracija elektrolita u g/l razmatrani su na brzine obrade i preseka. Rezultati su otkrili da elektromagnetni grafitni alat, alat sa stalnim magnetom i grafitne elektrode omogućuju brzinu obrade od 106,4%, 74,6% i 44,5% u odnosu na alat od nerđajućeg čelika pri sledećim uslovima glavnih faktora: 23 g/l, 15 V i 85%, redom.. Štaviše, grafitne i elektromagnetne grafitne elektrode su smanjile presek za 11,9% i 3,41%, redom, u odnosu na alat od nerđajućeg čelika pri sledećim uslovima: 8 V, 95% i 28 g/l. Pored toga, izvršeno je ispitivanje skenirajućim elektronskim mikroskopom da bi se identifikovao efekat magnetnog polja na radnu površinu.*

*Ključne reči: elektroda, elektromagnet, premaz, brzina obrade, presek.*

NAUČNI RAD